Sound transmission through finite lightweight multilayered structures with thin air layers

A. Dijckmans[a] and G. Vermeir
Afdeling Akoestiek en Thermische Fysica—Afdeling Bouwfysica, Katholieke Universiteit Leuven, Celestijnenlaan 200D, BE-3001 Heverlee, Belgium

W. Lauriks
Afdeling Akoestiek en Thermische Fysica, Katholieke Universiteit Leuven, Celestijnenlaan 200D, BE-3001 Heverlee, Belgium

(Received 23 February 2010; revised 19 July 2010; accepted 21 September 2010)

The sound transmission loss (STL) of finite lightweight multilayered structures with thin air layers is studied in this paper. Two types of models are used to describe the vibro-acoustic behavior of these structures. Standard transfer matrix method assumes infinite layers and represents the plane wave propagation in the layers. A wave based model describes the direct sound transmission through a rectangular structure placed between two reverberant rooms. Full vibro-acoustic coupling between rooms, plates, and air cavities is taken into account. Comparison with double glazing measurements shows that this effect of vibro-acoustic coupling is important in lightweight double walls. For infinite structures, structural damping has no significant influence on STL below the coincidence frequency. In this frequency region, the non-resonant transmission or so-called mass-law behavior dominates sound transmission. Modal simulations suggest a large influence of structural damping on STL. This is confirmed by experiments with double fiberboard partitions and sandwich structures. The results show that for thin air layers, the damping induced by friction and viscous effects at the air gap surfaces can largely influence and improve the sound transmission characteristics.
 [DOI: 10.1121/1.3500698]

PACS number(s): 43.55.Rg, 43.55.Ti, 43.55.Wk [LMW] Pages: 3513–3524

I. INTRODUCTION

In aerospace and car industry, economic and ecologic stimuli have increased the use of lightweight structures like composite sandwich panels. However, the combination of low mass and high stiffness typically results in a lower sound transmission loss (STL) over a large frequency band. Modern buildings are often required to make use of lightweight structures to a large extent. For this, several reasons can exist such as flexibility, cost, construction time, etc. Sufficient airborne and structureborne sound insulation throughout these buildings generally can only be created when multilayered structures are used. Specific type of multilayered structures often encountered in buildings are double walls, for example, double glazing and double gypsum board walls.

The vibro-acoustic behavior of multilayered structures and double walls has been studied analytically. Literature includes models based on the impedance approach,[1,2] the progressive-wave method,[3,4] and more recently, the transfer matrix method (TMM).[5,6] These methods assume infinite structures. In the TMM, different types of layers, such as elastic, poro-elastic, and fluid layers, can be easily incorporated. Statistical energy analysis (SEA) has also been used to calculate the transmission loss of double walls.[7,8] Craik *et al.*[9] experienced difficulties to properly describe the coupling between the cavity walls and air cavity, making STL predictions of cavity walls with empty cavity unreliable. Deterministic models have also been developed. These models take into account the finite dimensions of the structure. Also, the finite dimensions of the rooms on emitting and receiving side can be taken into account. Models based on well-known numerical methods, such as the finite element method (FEM) or the boundary element method (BEM), have been used.[10,11] These models typically are limited to the lower frequency range due to the high computation cost. Modal models have been developed which reduce the computation cost and therefore make simulations possible up to a higher frequency.[12–15] For single-layered walls, the consideration of full coupling between room modes and bending wave modes of the plate is not necessary in many cases.[16] For multilayered structures like double walls, the interaction between the vibrations of the panels and the acoustic pressure in the air gap cannot be neglected.

The sound transmission through double walls with large air cavities has been extensively investigated in literature—both numerically and experimentally. However, less is known about sound transmission through structures with thin air layers. Hongisto[17] has made an extensive study of double wall prediction models. Double walls with and without studs, and with and without cavity absorption were examined. Comparison between existing analytical models and experimental results showed a very high variation, even for the simplest type of walls without studs and cavity absorption. There is an obvious need for better understanding of the behavior of double walls with air gaps. The most problematic situation, which none of the models

[a]Author to whom correspondence should be addressed. Electronic mail: Arne.Dijckmans@bwk.kuleuven.be

investigated by Hongisto can deal with, is very thin and empty cavities (cavity depth < 30 mm). It is extremely difficult to determine the effective cavity absorption in such cases.

The effect of a thin air layer on the damping of a plate has been experimentally and analytically investigated by Önsay.[18] The attenuation and frequency shift of the plate's resonances were demonstrated for a cavity backed plate. Attention was given to the influence of the thickness of the air layer. When the air layer thickness is reduced, there is increased damping in the system. The viscous shear forces, induced in the air layer near the enclosing surfaces, become more effective at relatively smaller gaps, and thus increase the damping. Basten *et al.*[19,20] developed a modal model for double walls while taking into account the viscothermal effects in the air layer. It was shown that the damping of the so-called pumping modes of the plate can be largely increased by decreasing the thickness of the air layer. However, the influence of the viscothermal effects on the transmission loss calculations was very small in the considered frequency range (0–180 Hz). Only around the eigenfrequencies of the panel there are small differences between the results with and without taking into account viscothermal effects. The increased damping has only effect for resonant behavior of the panels and hardly influences the overall transmission loss, which is in the low-frequency region determined by the non-resonant or forced transmission (mass-law). More recently, Akrout *et al.*[21,22] studied the vibro-acoustic behavior of double panels and laminated double glazing with a finite element model, including the effects of viscosity and thermal conductivity of the cavity air. The numerical results showed the importance of the viscothermal effects in the case of thin air layers.

In this paper, double walls and multilayered walls with thin air layers are investigated. In Sec. II, two models are presented to describe the vibro-acoustic behavior of this type of structures. The TMM is used to describe plane wave propagation through infinite multilayered structures. A modal model is developed with the wave based method (WBM) to describe the direct transmission through multilayered walls, consisting of thin plates and air cavities, such as double walls, placed between two 3D rectangular rooms. Section III describes the experimental setups and test samples examined. In Sec. IV, the measurement results are shown and discussed. Comparison is made with TMM and WBM prediction results, to discuss the influence of vibro-acoustic coupling and damping. Especially the influence of extra damping—created by viscothermal effects in the air layer and friction at the cavity walls—on STL is discussed, by numerical and experimental examples.

II. VIBRO-ACOUSTIC MODELING

A. Transfer matrix method

The TMM is a general method for modeling acoustic fields in layered media which include fluid, elastic, and poro-elastic layers. Several acoustical applications of this method were published in literature.[6,23–25] The method assumes infinite layers and represents the plane wave propagation in different media in terms of transfer matrices. Interface matrices describe the boundary conditions between different layers depending on the nature of the two layers.

The TMM is a computational efficient technique to predict the sound transmission coefficient $\tau(\theta)$ of an infinite multilayered structure for plane wave excitation at an angle θ. To predict the STL of structures between two rooms, as measured in laboratory or *in situ*, one has to take an average transmission coefficient $\bar{\tau}$ over all incident angles. Diffuse field assumption leads to

$$\bar{\tau}(\omega) = \frac{\int_0^{90^\circ} \tau(\omega,\theta)\sin(\theta)\cos(\theta)\mathrm{d}\theta}{\int_0^{90^\circ} \sin(\theta)\cos(\theta)\mathrm{d}\theta}. \tag{1}$$

To give better agreement between measured and predicted STL, the integration is often limited to a maximum angle of incidence θ_{lim},[26]

$$\bar{\tau}(\omega) = \frac{\int_0^{\theta_{\mathrm{lim}}} \tau(\omega,\theta)\sin(\theta)\cos(\theta)\mathrm{d}\theta}{\int_0^{\theta_{\mathrm{lim}}} \sin(\theta)\cos(\theta)\mathrm{d}\theta}. \tag{2}$$

Typical values used for θ_{lim} lie between 78° and 85°. Kang *et al.*[27] have proposed a Gaussian distribution of incident energy $G(\theta)$,

$$G(\theta) = e^{-\beta\theta^2}. \tag{3}$$

β is a factor within the range of 1–2, depending on the source room characteristics.[27] This leads to following prediction formula for the average transmission coefficient:

$$\bar{\tau}(\omega) = \frac{\int_0^{90^\circ} G(\theta)\tau(\omega,\theta)\sin(\theta)\cos(\theta)\mathrm{d}\theta}{\int_0^{90^\circ} G(\theta)\sin(\theta)\cos(\theta)\mathrm{d}\theta}. \tag{4}$$

Villot *et al.*[28] have presented a spatial windowing technique of plane waves to take into account the finite size of a plane structure in sound radiation and sound transmission calculation. This finite size correction term takes into account the diffraction effects of the boundaries. Modal behavior of the structure is not incorporated.

For single-layered walls, the analytical TMM gives satisfactory results. Agreement between measurement and model is good—especially after applying correction terms like taking into account a maximum angle of incidence. Kurra and Arditi[29] have shown that the use of similar corrections for double walls with empty cavity and multilayered walls gives unrealistic simulation results.

B. Wave based method (WBM)

1. Problem definition

The WBM[13] is used to simulate the direct sound transmission through a rectangular structure, placed between two rectangular 3D rooms. The original model for single walls, developed by Osipov *et al.*,[30] has been extended to multilayered structures.[31] The geometry of the considered problem is shown in Fig. 1. The multilayered structure with

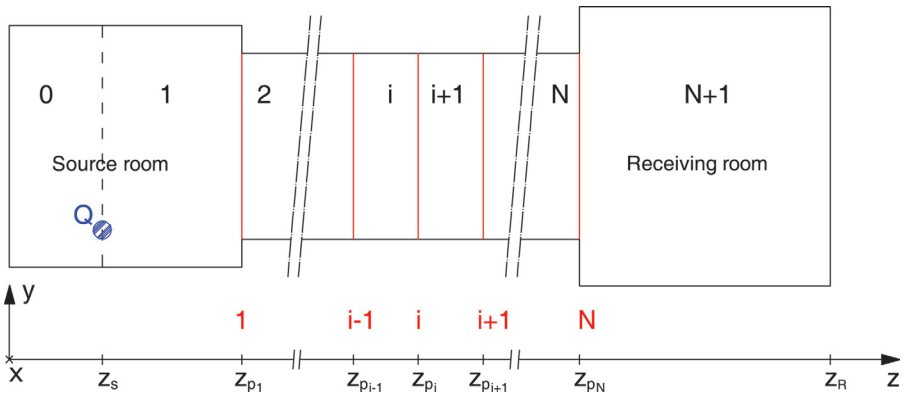

FIG. 1. (Color online) Geometry of the wave based model: A multilayered structure—composed of N rectangular plates, coupled by cavities—between two rectangular 3D rooms with rigid side and back walls.

dimensions L_{px} and L_{py} consists of N plates separated by air cavities. The side and back walls of the rooms are rigid, just as the side walls of the air cavities. The plates are simply supported. To calculate the airborne sound insulation, a harmonic volume point source is placed in the source room at position (x_s, y_s, z_s).

The source room is divided into two parts by a plane through the point source, parallel to the element. The steady-state acoustical pressure in each (sub)room and air cavity $\underline{p}_{a,i}$ $(i = 0 \ldots N + 1)$ is governed by the homogeneous Helmholtz equation,

$$\nabla^2 \underline{p}_{a,i}(x,y,z) + k_a^2 \underline{p}_{a,i}(x,y,z) = 0 \tag{5}$$

$k_a = \omega/c_{\text{air}}$ is the acoustic wavenumber in air, with ω the angular frequency, and c_{air} the speed of sound in air. In source and receiving room, uniform damping is introduced by making the acoustic wavenumber complex,[32]

$$\underline{k}_a = k_a\left(1 - j\frac{1}{2}\frac{2.2}{fT}\right), \tag{6}$$

where T is the reverberation time of the room, f is the frequency, $j = \sqrt{-1}$.

For acoustically thin plates, the transverse displacement $\underline{w}_i$ of the plates at position z_{pi} $(i = 1 \ldots N)$ fulfills Kirchhoff's thin plate bending wave equation,

$$\nabla^4 \underline{w}_i(x,y) - \underline{k}_{B,i}^4 \underline{w}_i(x,y) = \frac{\underline{p}_{a,i}(x,y,z_{pi}) - \underline{p}_{a,i+1}(x,y,z_{pi})}{\underline{B}_i'}, \tag{7}$$

where the bending wave number $\underline{k}_{B,i}$ and the plate bending stiffness $\underline{B}_i'$ are defined as

$$\underline{k}_{B,i} = \sqrt[4]{\frac{m_i'' \omega^2}{\underline{B}_i'}} \quad \text{and} \quad \underline{B}_i' = \frac{E_i h_i^3 (1 + j\eta_i)}{12(1 - \nu_i^2)}, \tag{8}$$

with $m_i'' = \rho_i h_i$ the surface mass density of plate i, h_i the plate's thickness. The material of plate i has a density ρ_i, a Young-modulus E_i, a loss factor η_i, and a Poisson coefficient ν_i.

2. Field variable expansions

The acoustic pressures are approximated in terms of the following acoustic wave function expansion:

$$\underline{p}_{a,i}(x,y,z) = \sum_{m=0}^{M}\sum_{n=0}^{N} (e^{-j\underline{k}_{zimn}z}\underline{A}_{imn} + e^{j\underline{k}_{zimn}z}\underline{B}_{imn}) \cos\left(\frac{m\pi}{L_{x,i}}x\right) \cos\left(\frac{n\pi}{L_{y,i}}y\right), \tag{9}$$

where

$$\underline{k}_{zimn} = \sqrt{\underline{k}_a^2 - \left(\frac{m\pi}{L_{x,i}}\right)^2 - \left(\frac{n\pi}{L_{y,i}}\right)^2}. \tag{10}$$

$L_{x,i}$ and $L_{y,i}$ are the cross-sectional dimensions of the respective room or cavity, m and n are integers. The wave functions are exact solutions of the homogeneous Helmholtz equation (5). The time dependence $e^{j\omega t}$ has been omitted throughout this paper.

Using Euler's equation, Eq. (9) leads to following wave function expansion for the air particle displacement in the z-direction:

$$\begin{aligned}\underline{w}_{a,i}(x,y,z) &= \frac{1}{\omega^2 \rho_{\text{air}}}\frac{\partial \underline{p}_{a,i}}{\partial z} \\ &= -\frac{j}{\omega^2 \rho_{\text{air}}}\sum_{m=0}^{M}\sum_{n=0}^{N} \underline{k}_{zimn} \\ &\quad \times (e^{-j\underline{k}_{zimn}z}\underline{A}_{imn} - e^{j\underline{k}_{zimn}z}\underline{B}_{imn}) \\ &\quad \times \cos\left(\frac{m\pi}{L_{x,i}}x\right) \cos\left(\frac{n\pi}{L_{y,i}}y\right),\end{aligned} \tag{11}$$

with ρ_{air} the density of air.

Also for the transverse displacement of the plates, a field variable expansion is used,

$$\underline{w}_i(x,y) = \sum_{p=1}^{P}\sum_{q=1}^{Q} \underline{C}_{ipq} \sin\left(\frac{p\pi}{L_{px}}x\right) \sin\left(\frac{q\pi}{L_{py}}y\right). \tag{12}$$

3. Continuity and boundary conditions

The proposed pressure expansions satisfy *a priori* the rigid wall boundary conditions. The plate displacement

expansions satisfy *a priori* the simply supported boundary conditions. The unknown pressure and plate amplitudes $\underline{A}_{imn}$, $\underline{B}_{imn}$, and $\underline{C}_{ipq}$ are determined by the boundary conditions at back walls and the continuity conditions. At the rigid back walls of source ($z = 0$) and receiving room ($z = z_R$), the air particle displacement must be zero,

$$\underline{w}_{a,0}(x,y,0) = \underline{w}_{a,N+1}(x,y,z_R) = 0. \tag{13}$$

The coupling conditions at the source plane ($z = z_s$) can be written as follows:

$$\begin{aligned} &\underline{p}_{a,0}(x,y,z_s) = \underline{p}_{a,1}(x,y,z_s), \\ &j\omega\underline{w}_{a,0}(x,y,z_s) + \delta(x_s,y_s) = j\omega\underline{w}_{a,1}(x,y,z_s), \end{aligned} \tag{14}$$

where δ is the Dirac function. At the plates surfaces ($z = z_{pi}$), continuity of transverse displacement is imposed,

$$\begin{aligned} &\underline{w}_i(x,y) = \underline{w}_{a,i}(x,y,z_{pi}) \\ &\underline{w}_i(x,y) = \underline{w}_{a,i+1}(x,y,z_{pi}), \quad i = 1 \ldots N. \end{aligned} \tag{15}$$

The thickness of the plates is neglected according to thin plate theory.

The coupling and boundary conditions (13)–(15), together with the plate impedance Eq. (7), are expressed in weighted residual formulations.

$$\int_0^{L_{x,i}} \int_0^{L_{y,i}} R_j^{(a_i)} \varphi_{aimn}(x,y)\mathrm{d}x\mathrm{d}y = 0 \tag{16}$$

$$\int_0^{L_{px}} \int_0^{L_{py}} R^{(p_i)} \varphi_{pmn}(x,y)\mathrm{d}x\mathrm{d}y = 0. \tag{17}$$

$R_j^{(a_i)}$ is the error function related to the respective boundary conditions (13) and coupling conditions (14) and (15).

$$\begin{aligned} R_1^{(a_0)} &= \underline{w}_{a,0}(x,y,0), \\ R_2^{(a_{N+1})} &= \underline{w}_{a,N+1}(x,y,z_R), \\ R_3^{(a_0)} &= \underline{p}_{a,0}(x,y,z_s) - \underline{p}_{a,1}(x,y,z_s), \\ R_4^{(a_1)} &= j\omega\underline{w}_{a,0}(x,y,z_s) + \delta(x_s,y_s) - j\omega\underline{w}_{a,1}(x,y,z_s), \\ R_5^{(a_i)} &= \underline{w}_{a,i}(x,y,z_{pi}) - \underline{w}_i(x,y), \\ R_6^{(a_{i+1})} &= \underline{w}_{a,i+1}(x,y,z_{pi}) - \underline{w}_i(x,y). \end{aligned} \tag{18}$$

$R^{(p_i)}$ is the error function following from Eq. (7).

$$\begin{aligned} R^{(p_i)} = {} & \nabla^4 \underline{w}_i(x,y) - \underline{k}_{B,i}^4 \underline{w}_i(x,y) \\ & - \frac{\underline{p}_{a,i}(x,y,z_{pi}) - \underline{p}_{a,i+1}(x,y,z_{pi})}{\underline{B}_i'}. \end{aligned} \tag{19}$$

The wave functions used in the field variable expansions are used as weighting functions (Galerkin's choice procedure),

$$\begin{aligned} \varphi_{aimn} &= \cos\left(\frac{m\pi}{L_{x,i}}x\right)\cos\left(\frac{n\pi}{L_{y,i}}y\right), \\ \varphi_{pmn} &= \sin\left(\frac{m\pi}{L_{px}}x\right)\sin\left(\frac{n\pi}{L_{py}}y\right). \end{aligned} \tag{20}$$

With Eq. (16), the pressure amplitudes $\underline{A}_{imn}$ and $\underline{B}_{imn}$ can be written in function of the coefficients $\underline{C}_{ipq}$. Equation (17) finally results in a set of linear equations in the unknown plate amplitudes $\underline{C}_{ipq}$.

4. Truncation criteria

The number of wave functions M, N, P, and Q used in the expansion series (9) and (12) is determined by following frequency-dependent truncation criteria,

$$\omega_{aiMN} \simeq \omega_{piPQ} \geq a_{tr}\omega \tag{21}$$

where ω_{aiMN} and ω_{piPQ} are the eigenfrequencies associated with the room- and platemodes;

$$\omega_{aiMN} = c_{\mathrm{air}}\sqrt{\left(\frac{M\pi}{L_{x,i}}\right)^2 + \left(\frac{N\pi}{L_{y,i}}\right)^2}, \tag{22}$$

$$\omega_{piPQ} = \sqrt{\frac{B_i'}{m_i''}}\left(\left(\frac{P\pi}{L_{px}}\right)^2 + \left(\frac{Q\pi}{L_{py}}\right)^2\right). \tag{23}$$

In the simulations, a truncation factor $a_{tr} = 2.0$ is used. In the low-frequency range, a minimal number of wave functions is selected to assure convergence.[13]

5. Calculation of STL

The STL is determined by following measurement formula:

$$\mathrm{STL} = L_{pe} - L_{pr} + 10\log\frac{S}{A_r}. \tag{24}$$

The sound pressure levels in emitting and receiving room L_{pe} and L_{pr} are calculated by analytical integration of the acoustic pressure over the respective room volumes. S is the surface area of the element and $A_\mathrm{r} = 0.16V_r/T_r$ the absorption area of the receiving room, with V_r the volume and T_r the reverberation time.

STL is calculated at 81 frequencies per third octave band. The average STL in each frequency band is calculated from the summated sound pressure levels $L_{p,1/3\ \mathrm{octave}}$

$$L_{p,1/3\ \mathrm{octave}} = 10\log\left(\sum_{i=1}^{81} 10^{L_{p,i}/10}\right). \tag{25}$$

III. EXPERIMENTAL WORK

A. Measurement setup

1. Sound transmission loss

The airborne sound insulation of different test panels was measured in third octave bands with the pressure method

according to ISO 140-3 in the reverberation chambers of the Laboratory of Acoustics at the K.U.Leuven.

$$\mathrm{STL} = L_{pe} - L_{pr} + 10\log\frac{S}{A_r}, \tag{26}$$

where L_{pe} and L_{pr} are the mean pressure levels in third octave bands in emitting and receiving room, respectively (averaged over six microphone positions in each room). S is the surface area of the test sample. Double glazing, three types of double fiberboard walls, and two types of sandwich panels were measured in a small transmission opening with dimensions 1.25 m × 1.50 m. A third type of sandwich panel was measured in the large transmission opening with dimensions 3.25 m × 2.95 m (see Sec. III B). The absorption A_r is determined by measuring the mean reverberation time T_r of the receiving room over six microphone positions.

Each reverberation chamber has a volume V of 87 m^3. The cut-off frequency $f = \sqrt{c_{\mathrm{air}}^3 T_r/8.8\pi V}$ is around 160 Hz. The common wall in the laboratory is not parallel with the back walls.

2. Loss factor

The total loss factor η of the installed test samples was measured by means of the integrated impulse response method. The impulse response of the structure is measured with accelerometers (Dytran type 3100D24) and hammer excitation. The averaged value of 24 decay curves is taken, four measurement points × three excitation points × two decays per point. The structural reverberation time T of the samples is then obtained from the measured impulse response functions according to ISO 3382. The total loss factor is retrieved from the following formula:

$$\eta = \frac{2.2}{fT}. \tag{27}$$

B. Test samples

1. Double glazing 6(12)8 mm

A simple double glazing, without frame, is placed on one side of the small transmission opening. The glass panes have thicknesses of 6 and 8 mm, resulting in coincidence frequencies of approximately 2130 and 1600 Hz, respectively. The width of the air gap is 12 mm.

2. Double fiberboard walls

A measurement series with double fiberboard walls was set up in the small transmission opening.[33] For the double-leaf partitions, two types of fiberboard were used. The first type of fiberboard has a smooth surface. The second type has rough surfaces. All the plates have a thickness of 9.5 mm. The fiberboard with smooth surface has a surface mass of approximately 7.1 kg/m^2, the rough fiberboard weighs approximately 6.5 kg/m^2. The two plates are separated from each other with soft strips at the edges of the plates (see Fig. 6) to create an air cavity of, respectively, 3, 6, and 12 mm depth and minimize the mechanical coupling between the two plates. The influence of cavity absorption was further examined by placing a 2 mm thick felt layer inside the air cavity. The felt layer was loosely attached to one of the plates (fiberboard with rough surfaces). As a reference, the STL of the single fiberboard panels was also measured.

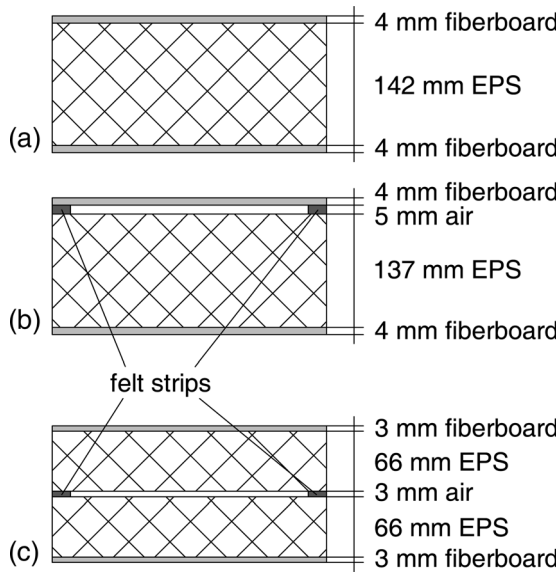

FIG. 2. Schematic sections of EPS sandwich panels: (a) Type 1, (b) Type 2, and (c) Type 3.

3. EPS sandwich panels

Finally, three types of sandwich panels with a core of expanded polystyrene (EPS) were investigated (see Fig. 2). As a reference, the STL of a basic EPS sandwich panel with dimensions 1.50 m × 1.25 m and thickness 150 mm was measured. The panel consists of a core of EPS with a 4 mm fiberboard plate glued on each side (sandwich type 1). In the second configuration, one of the fiberboard plates is decoupled from the EPS core with 5 mm thick strips of felt at two edges, creating a thin air cavity between fiberboard plate and EPS (sandwich type 2). The second EPS panel had dimensions 1.50 m × 1.25 m and a total thickness of 150 mm. A third type of sandwich panel was measured in the large transmission opening (3.25 m × 2.95 m). Three 1.02 m × 2.95 m panels were placed in the opening. The gaps at the edges and between the panels were filled with mineral wool and covered with plasterboard. The panels had a total thickness of 143 mm. The fiberboard plates, glued to the EPS core, had a thickness of 3 mm. The core consists of two 67 mm EPS layers, separated by three felt layers, so creating a 3 mm thick air layer (sandwich type 3).

IV. DISCUSSIONS

A. Double glazing

1. Vibro-acoustic coupling

In Fig. 4(a) the measured STL of the double glazing 6(12)8 mm is compared with TMM simulation results. All

TABLE I. Material data used in simulations.

	ρ (kg/m^3)	E (Pa)	η (−)	ν (−)
Glass	2500	$62\,000 \times 10^6$	…[a]	0.24
Fiberboard (smooth)	750	3500×10^6	…[a]	0.46
Fiberboard (rough)	675	3500×10^6	…[a]	0.46
Fiberboard (sandwich)	850	3500×10^6	0.01	0.46
EPS	15	13×10^6	0.05	0.10

[a]Measured values, see Fig. 3.

TMM simulations assume diffuse sound field excitation, $\theta_{\text{lim}} = 90°$. The material properties used for the simulations are given in Table I. For the loss factor, the measured values are used [see Fig. 3(a)]. No cavity damping is taken into account. TMM simulation for infinite structures and diffuse sound field excitation shows a large underestimation of STL in a broad frequency band between the mass-spring-mass-resonance of the structure around 200 Hz and the coincidence frequencies around 2000 Hz. Even after applying correction terms for the diffraction effects by spatially windowing the results,[28] or a Gaussian distribution of incident energy,[27] the discrepancy remains.

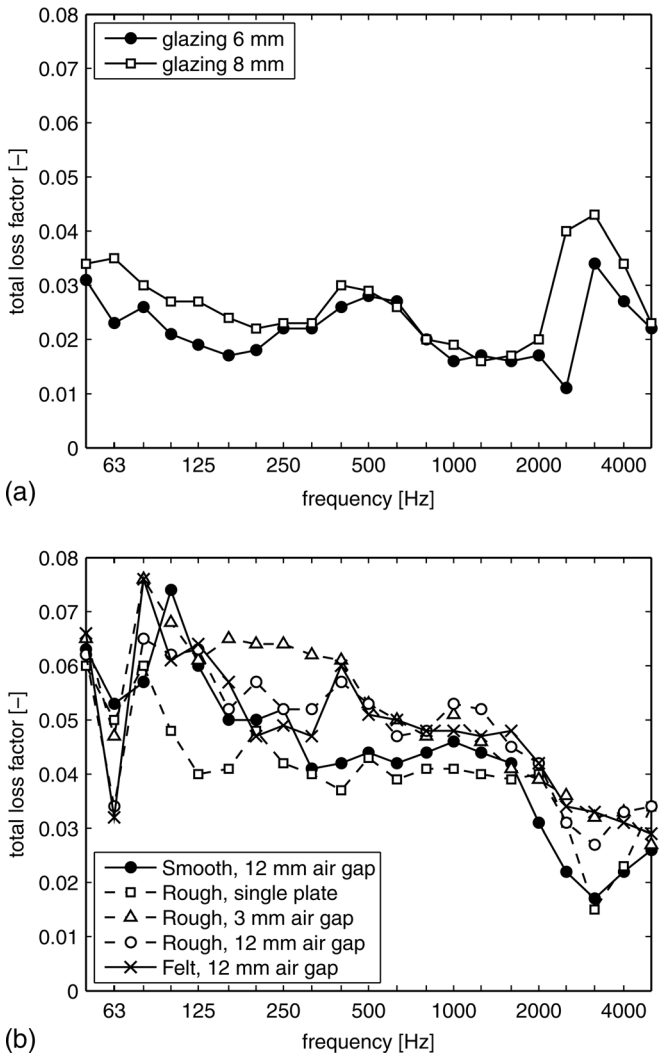

FIG. 3. Measured values of total loss factor. (a) Double glazing, (b) Fiberboard walls.

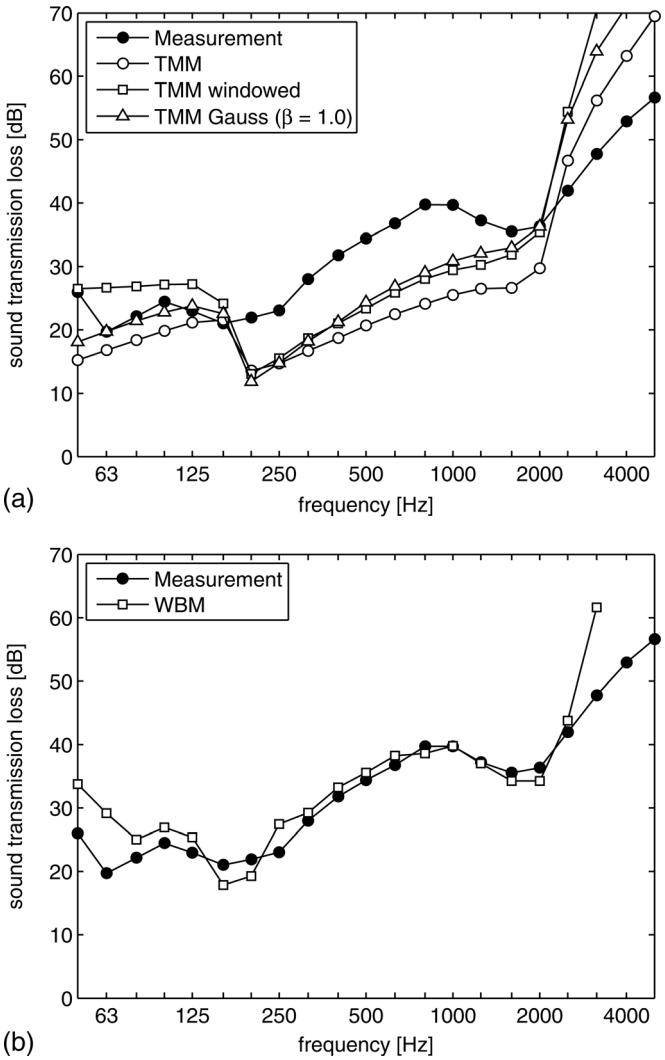

FIG. 4. STL of double glazing 6(12)8 mm with dimensions 1.5 m × 1.25 m. Measurement and simulations (without cavity absorption). (a) TMM ($\theta_{\text{lim}} = 90°$), (b) WBM.

Figure 4(b) shows WBM simulation results for the double glazing structure. The reverberant rooms of the laboratory are approximated by rectangular rooms. The dimensions used for source and receiving room are 5.11 m × 4.11 m × 4.15 m and 5.08 m × 4.10 m × 4.18 m, respectively. A representative value of 1.5 s is taken for the reverberation time of the rooms. The agreement between simulation and measurement result is good over a broad frequency range. Above the coincidence dip around 2000 Hz, the WBM still overestimates the STL. This can be due to the fact that flanking transmission at the edges, which is not taken into account, determines the sound transmission. In the measurement result, the dip around the mass-spring-mass-resonance frequency is less pronounced and broader compared to WBM simulation results. The underestimation in STL is, however, smaller compared with TMM simulations.

In this case, taking into account the modal behavior of the structure and the rooms is important. The assumption of a diffuse sound field excitation made in TMM is not realistic. Especially for double walls, where sound transmission is strongly dependent on angle of incidence, it is important to

take into account the source room characteristics.[34] The finite dimensions of the glass panes and the air layer in between, results in a specific vibro-acoustic coupling mechanism. For infinite structures, as assumed in TMM, the air layer stiffness, as seen by the glass panes, is strongly dependent on the angle of incidence θ of the plane wave. Therefore, the mass-spring-mass frequency f_{msm} is also dependent on θ.[4]

$$f_{\mathrm{msm}}(\theta) = \frac{1}{\cos\theta} f_{\mathrm{msm},0} = \frac{1}{\cos\theta}\frac{1}{2\pi}\sqrt{\frac{\rho_{\mathrm{air}} c_{\mathrm{air}}^2}{d}\left(\frac{1}{m_1''}+\frac{1}{m_2''}\right)}, \quad (28)$$

where d is the cavity depth, m_1'' and m_2'' the surface mass of the panels. The lowest mass-spring-mass-resonance frequency is obtained at normal incidence ($\theta = 0$). The air stiffness increases with increasing angle of incidence. This results in a very broad mass-spring-mass-resonance dip for infinite structures. In real structures, this unrealistic increase of air layer stiffness is not encountered, because the air cavity has finite lateral dimensions. The amount of cavity modes with grazing incident angle is limited. As a result, the stiffness of the air cavity is lower than calculated for infinite structures.

2. Structural damping

The influence of the total loss factor η of the glass panes on STL simulation results is shown in Fig. 5. TMM simulations for infinite structures predict a minor influence of structural damping on the STL. Only around the coincidence dips of the glass panes (1600 and 2130 Hz), there is an increase in STL by increasing the total loss factors of the panels. In the low-frequency range and around the mass-spring-mass-resonance frequency of 200 Hz, damping has no influence on TMM prediction results.

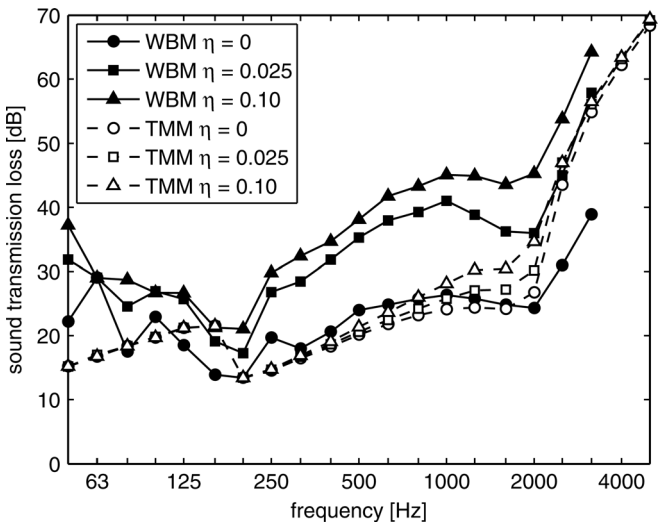

FIG. 5. Influence of structural damping on STL of double glazing 6(12)8 mm with dimensions 1.5 m × 1.25 m. TMM ($\theta_{\mathrm{lim}} = 90°$) and WBM simulations (no cavity absorption).

The influence of total loss factor on WBM simulations is larger, especially between the mass-spring-mass-resonance frequency and the coincidence dips. WBM simulation results with no structural damping ($\eta = 0$) predict STL of the same order as TMM. When structural damping is introduced, the WBM predicts a significant increase in STL in the entire frequency range of interest. Even a little amount of damping ($\eta = 0.025$) already increases STL above the mass-spring-mass-resonance frequency by 10–15 dB.

In the TMM, infinite structures are assumed. Sound transmission below coincidence is dominated by forced or non-resonant transmission.[4] This mass-law behavior is independent of the total damping of the structure. The damping becomes important around and above the critical frequency, where resonant transmission by coincidence is dominant. The WBM describes the sound transmission in function of excitation and radiation of structural modes. The amplitudes of the resonant modes are largely influenced by the total damping. As frequency averaged STL values are dominated by the dips at resonances, damping can significantly influence STL values of real structures with finite dimensions, also below the critical frequency.

3. Cavity absorption

In the TMM and WBM simulations for the double glazing, no cavity absorption is taken into account. The discrepancy between measurement results and infinite layer simulations in the frequency range between the mass-spring-mass-resonance dip and the coincidence dip can be explained by the finite dimensions. In literature,[14,27,34–36] one often introduces cavity damping or cavity absorption when modeling double walls with empty cavities. However, sound absorption coefficients which are higher than the physical sound absorption coefficients have to be assumed for infinite models. The need for this unrealistic high cavity damping is not encountered in the wave based model.

B. Double fiberboard walls

1. Measurement results

The STL measurement results for the double fiberboard partitions are shown in Fig. 6.

The fiberboard partitions with smooth surface inside the cavities show typical results, comparable with measurement results of double glazing [see Fig. 6(a)]. In the low-frequency region, the STL increase from single to double walls is approximately 6 dB, according to the mass law. Depending on the cavity depth, a mass-spring-mass-resonance dip is visible in the middle frequency range. The resonance frequency decreases when the cavity depth increases according to classical double wall theory. Around the resonance dip, the STL of the double partitions is lower than the single-leaf partition STL. At higher frequencies, the double-wall STL surpasses that of the single-leaf partition. The improvement is larger for wider cavities, as the double wall effect starts from the mass-spring-mass-resonance frequency on. Around 3150 Hz, the coincidence dip of the fiberboard plates is clearly visible.

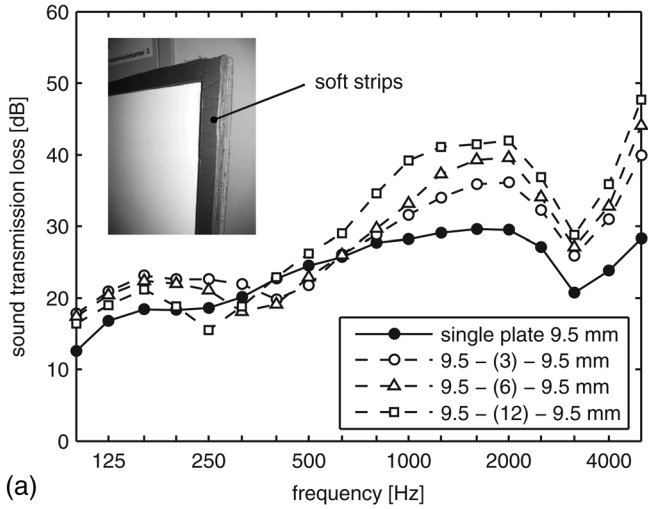

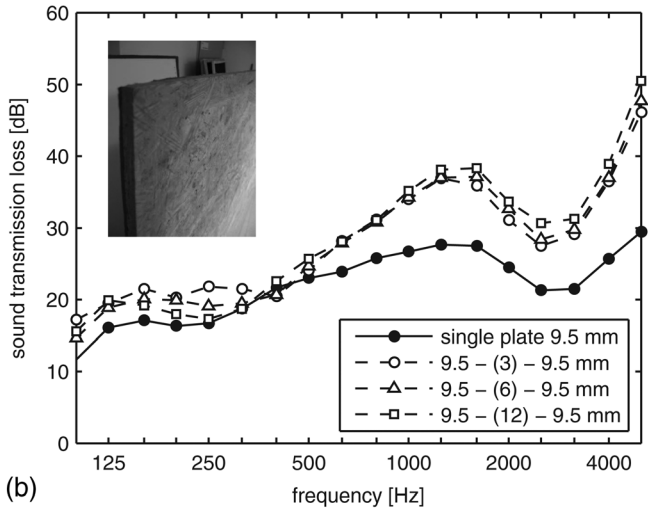

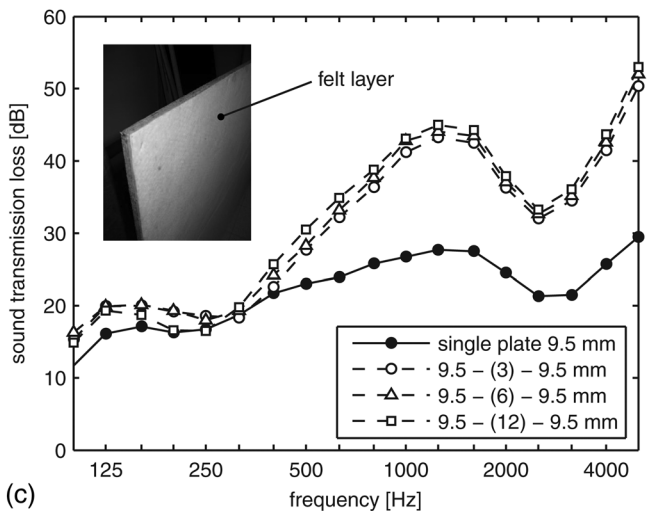

FIG. 6. Measured STL of single and double-leaf fiberboard partitions. (a) Type 1: Smooth surface, empty cavity. (b) Type 2: Rough surface, empty cavity. (c) Type 3: Rough surface, 2 mm felt layer in cavity.

When the fiberboard partitions have a rough surface, the improvement in transmission loss above the mass-spring-mass-resonance frequency is almost independent of the air cavity depth [see Fig. 6(b)]. Only around the coincidence frequency minor improvements show up when the cavity depth is increased. While the double partitions with smooth surface show a clear resonance dip, the rough finishing makes this dip less prominent. This may be linked to an increased amount of edge damping, resulting in a higher total loss factor [see Fig. 3(b)]. As a result, the STL of the double partitions is higher than that of the single fiberboard in almost all frequency bands.

The double fiberboard walls with a 2 mm thick felt layer inside the cavity show a similar behavior [see Fig. 6(c)]: Minor influence of cavity depth and a higher transmission loss compared to the single fiberboard in all frequency bands. As the felt layer introduces more absorption inside the cavity, the improvement in transmission loss above the mass-spring-mass-resonance frequency is larger compared to empty cavity results.

2. Simulations

The material properties used for the fiberboards in TMM and WBM simulations are given in Table I. No cavity absorption is taken into account. The simulations for the single fiberboard partition in Fig. 7(a) show good agreement

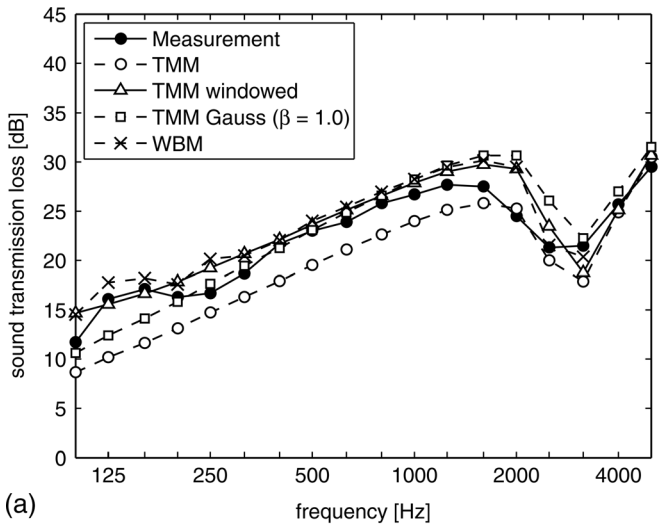

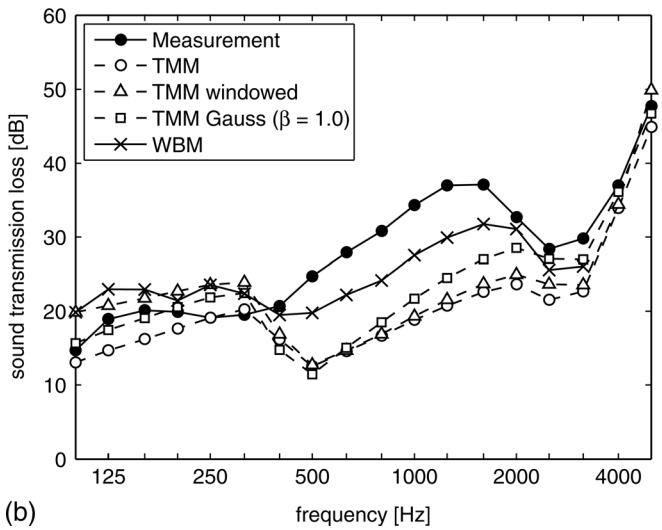

FIG. 7. STL measurement vs TMM ($\theta_{\text{lim}} = 90°$) and WBM simulations (no cavity absorption). (a) Single fiberboard wall, rough surfaces. (b) Double fiberboard wall, rough surfaces, 6 mm air gap.

with measurement results, although it is important in TMM to take into account the finite dimensions by spatially windowing the results. In the mid- and high-frequency ranges, TMM with spatial windowing gives almost identical third octave STL values as WBM. The infinite layer simulations can also be approved by applying a Gaussian distribution of incident energy. An optimal value of $\beta = 1.0$ is used in Eq. (3), higher values of β give an overestimation of STL.

For the double fiberboard walls [see Fig. 7(b)], the TMM predicts a large dip in sound insulation around the theoretical mass-spring-mass-resonance frequency (around 430 Hz). As this phenomenon is far less prominent in measurements, a large discrepancy exists between measurements and simulations in the mid-frequency range. Simulation results show that this discrepancy cannot be explained by taking into account a Gaussian distribution of incident energy or the finite dimensions by spatially windowing the results. This problem was already encountered with the double glazing structure (see Sec. IV A 1). In that case, taking into account the modal behavior of rooms, plates, and air cavity in the WBM gave excellent agreement with measurement. For the fiberboard walls, the modal behavior can only partly explain the discrepancy. The discrepancy between WBM and measurement is less compared with TMM, but there is still an underestimation in the mid-frequency range. Other effects encountered in this type of double walls with thin air layers must be taken into account.

3. Cavity absorption

When modeling double walls, it is important to take into account the cavity absorption.[2,14,26,27,34–36] The problem of modeling cavity absorption was already mentioned by Hongisto.[17] The most problematic situation that none of the models investigated by Hongisto can deal with is very thin and empty cavities ($d < 30$ mm). In this case, the surface absorption of the panels can have a strong effect even at low frequencies because the in-plane sound fields cannot propagate freely in the cavity due to wall friction. It is extremely difficult to determine the effective cavity absorption in such cases. The application of nominal panel absorption coefficients leads to strong underestimation of STL in the models investigated by Hongisto.

One difficulty in the determination of the effective absorption is the presence of viscothermal damping. Due to the viscous and thermal effects, energy is dissipated in the air layer. The viscous shear and thermal conduction remove energy from the vibration of the plates, which is experienced as damping. For lightweight double wall panels with thin air layers, this viscothermal damping level can be much higher than structural damping in the plates and radiation damping due to sound radiation to the environment.[20–22]

As seen in the previous section, the transmission loss measurements for partitions with a rough surface show similar behavior to the double walls with felt inside the cavity. This shows that for thin air layers, not only absorptive material inside the cavity but also absorption at the cavity walls strongly influences transmission loss. The amount of viscous damping is related to the roughness of the surfaces. This extra damping in the air layer, located at the surfaces of the plate, is simulated by an absorption α_s of the cavity walls. To model the absorption α_s in TMM and WBM, the absorption is uniformly distributed over the air cavity (with volume V and depth d), by making the wavenumber in air $\underline{k}_a$ complex:

$$\underline{k}_a = \frac{2\pi f}{c_{\text{air}}}\left(1 - j\frac{1}{2}\frac{2.2}{fT_{\text{eq}}}\right), \tag{29}$$

where

$$T_{\text{eq}} = \frac{0.16V}{A_{\text{eq}}} = \frac{0.16d}{2\alpha_s}, \tag{30}$$

with T_{eq} the equivalent reverberation time and A_{eq} the equivalent absorption area of the cavity. To validate this assumption, comparison is made with the multiple reflection theory.[2] In this model, sound incident on an infinite double panel is treated as a ray which is successively reflected by and transmitted through each panel. The absorption coefficient of the cavity walls is taken into account locally, by reducing the fraction reflected by a panel with a factor $(1 - \alpha_s)$. Figure 8 shows that distributing the absorption over the cavity is a good approximation in this case for thin air layers.

Figure 9 shows the simulation results for the double fiberboard partitions with rough surfaces (6 mm air gap) when taking into account a frequency independent absorption factor $\alpha_s = 0.02$. Low values of cavity absorption, which can be physically explained by friction at the surfaces and viscothermal effects in the air layer, already significantly increase the WBM predictions for transmission loss. WBM predicts similar behavior by increasing the structural damping (see Sec. IV A 2). In the case of damping in the air layer, the TMM also predicts a significant increase in STL, in contrast with the effect of structural damping. The resonances in the air gap are damped. The air layer damping especially reduces the obliquely incident waves.

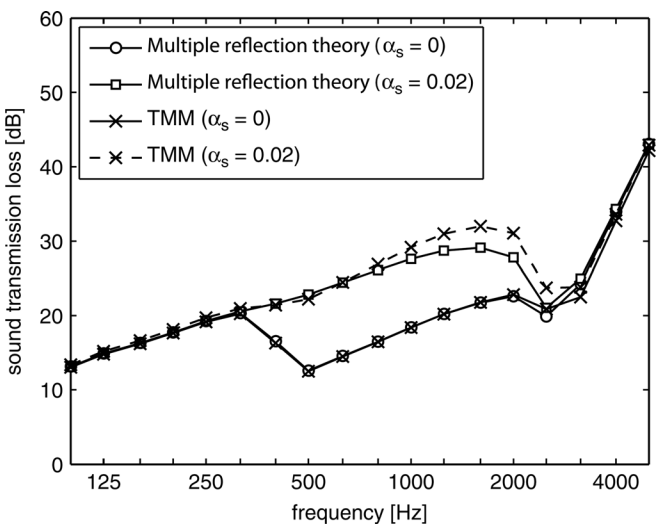

FIG. 8. Effect of cavity absorption: Local absorption vs uniform fluid damping (double fiberboard wall, rough surface, 6 mm air gap).

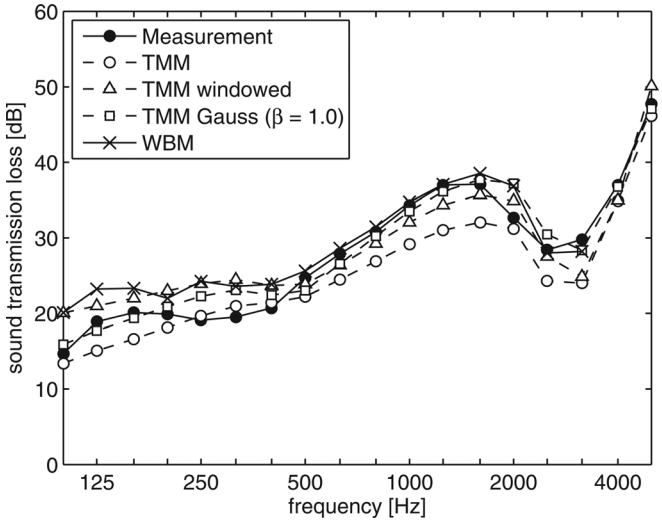

FIG. 9. Double fiberboard wall, rough surface, 6 mm air gap. Simulations with cavity absorption ($\alpha_s = 0.02$).

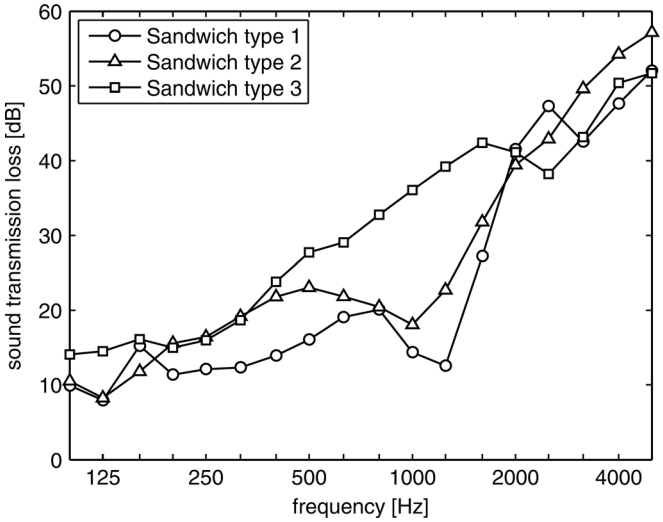

FIG. 10. Measured STL of EPS sandwich panels.

For the fiberboard walls with smooth surface (6 mm air gap), a value of 0.01 for α_s gives the best agreement between measurement and simulation results (which are not shown here for brevity).

Basten *et al.*[19] and Basten[20] showed that viscothermal effects in a thin air layer could largely increase plate damping, but hardly influence transmission loss. Minor influence was seen around the resonance dips of the structure. However, only frequencies up to 180 Hz were investigated and damping introduced by friction at the surfaces was not incorporated in the model. In the mid-frequency range, the extra damping by viscothermal effects and friction damping can significantly increase transmission loss. Damping decreases the dips at the plate's and cavity's resonances. In these frequency bands, there are sufficient eigenfrequencies to give damping a significant effect on the frequency-averaged transmission loss.

C. Sandwich panels

1. Measurement results

In Fig. 10, the STL measurements for the three types of sandwich panels are shown.

The transmission loss of the standard sandwich panel (type 1) is low in a wide frequency range, resulting in a low single noise rating R_w. At low frequencies till approximately 250 Hz, the transmission loss is restricted by the low surface mass (approximately 9.0 kg/m^2). In the mid-frequency range (250–1000 Hz), sound transmission is dominated by shear wave coincidence in the EPS core.[4] This is the so-called shear-controlled frequency region. Around 1000–1250 Hz, the dilatation resonance of the two plates on the EPS core results in a dip in transmission loss. Above this mass-spring-mass-resonance frequency, the STL significantly increases, until the thickness resonance dip (of longitudinal waves in the EPS) around 3150 Hz.

Decoupling one of the sandwich plates (type 2) improves the transmission loss in almost the entire frequency range of interest. The mass-spring-mass frequency is lower compared to the first sandwich panel with both plates glued to the EPS. This can be explained by the stiffening effect of the glued plates on the core[25] for sandwich panel type 1. The thin air layer has a positive effect, increasing R_w by 5 dB. The improvement in transmission loss is largest in the shear-controlled frequency range and around the mass-spring-mass-resonance frequency.

When a thin air layer is introduced in the middle of the EPS core (type 3), the improvement is even larger. Although the total thickness of sandwich panel 3 is smaller and the fiberboards are thinner (3 mm compared to 4 mm), the single noise rating is increased by more than 10 dB. The resonance dip around 1000–1250 Hz is completely eliminated.

2. TMM simulations

The sandwich panels are modeled with the TMM. The EPS core is modeled as an elastic layer. The material properties used in the simulations are given in Table I. These are optimized for the STL results of the first sandwich panel (see Fig. 11). The

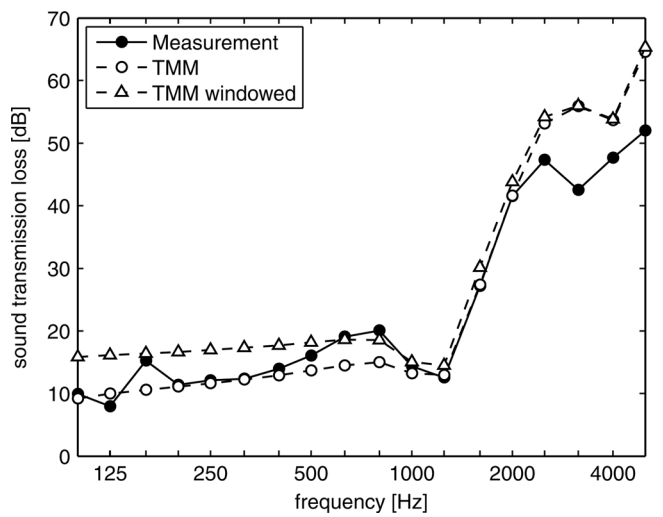

FIG. 11. EPS sandwich panel type 1: TMM simulations ($\theta_{\lim} = 90°$).

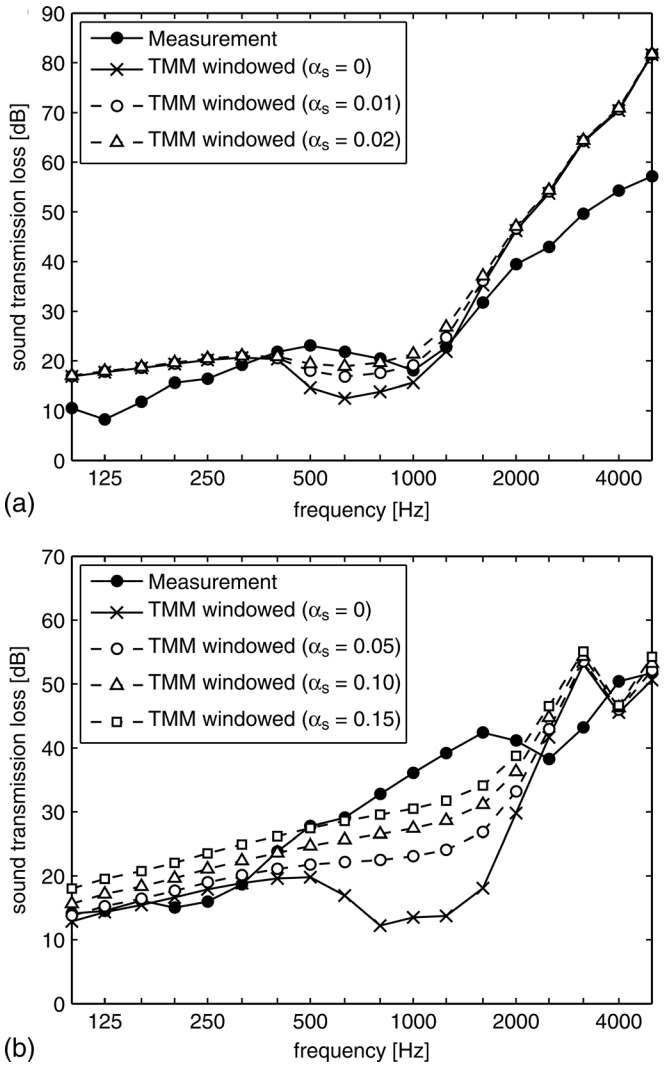

FIG. 12. EPS sandwich panels: Influence of cavity absorption on TMM simulations ($\theta_{\text{lim}} = 90°$, with spatial windowing). (a) Type 2 (1.25 m × 1.50 m), (b) Type 3 (3.06 m × 2.95 m).

agreement between measurement and simulation is good over a broad frequency range.

The same material properties are used for STL simulations of sandwich panels 2 and 3. Figure 12 shows the results with spatial windowing. When no cavity absorption is taken into account, the TMM predicts a dip in sound insulation around the theoretical mass-spring-mass-resonance frequency on the thin air layer. As this phenomenon is not seen in the measurements, a large discrepancy exists between measurement and simulation in the mid-frequency range, especially for sandwich panel 3.

3. Viscous damping

No dilation resonance dip is visible in the STL measurement of sandwich panel 3. This can be related to the presence of extra damping in the thin air layer. As seen in Sec. IV B 3, in a thin air layer the damping can be significant due to viscothermal effects in the air layer and friction with the cavity walls.

In the second panel, this phenomenon is also visible, but less clear. The absorption created by friction in the air cavity between plate and core is smaller. The surface of the plate is less rough than that of the EPS. In sandwich panel 3, two EPS surfaces are in contact with the air layer, whereas in sandwich panel 2 only one.

Figure 12 shows the influence of cavity absorption on TMM simulation results for sandwich panels 2 and 3. The dip between 500 and 1000 Hz, which was predicted for panel 2 with no cavity absorption, is less pronounced when little amounts of cavity absorption are included. The discrepancy between measurement and TMM simulation for STL of panel type 3 can be partly explained by absorption in the thin air layer. However, much larger values of surface absorption have to be used to reduce the underestimation in the simulations.

As shown for the double walls investigated, the predicted influence of structural damping on STL was larger in the wave based model, compared to TMM simulations. By taking into account the modal behavior of the sandwich panels and air cavities, the discrepancy between measurement and simulations could probably be further explained. Further numerical investigations on the modal behavior of finite, multilayered structures with thin air layers could be useful for better understanding.

V. CONCLUSIONS

Transmission loss of finite lightweight double walls and multilayered structures with thin air layers is investigated in this paper. The direct transmission between two rooms through double walls is described by a wave based model, where the full coupling between the room modes, air cavity modes, and bending wave modes of the plates is taken into account. Sound transmission through multilayered structures is predicted by a TMM. Results with double glazing show that it is important to take into account the modal behavior of lightweight double walls with thin air layers. TMM predictions, where infinite structures are assumed, largely underestimate STL in the mid-frequency range between the mass-spring-mass-resonance frequency and coincidence frequency. The need of introducing fictitious cavity damping in analytical models for a better agreement with measurement results is not necessary when taking into account the finite dimensions. Furthermore, STL of multilayered structures with thin air layers can be increased in this frequency range by adding structural damping or damping in the air layer. The cavity absorption in thin air layers is the result of viscothermal damping and friction at the cavity surfaces. WBM simulation results have shown that a little amount of absorption can already largely improve STL. Experiments on double fiberboard walls and EPS sandwich panels have also confirmed the significant influence of absorption in thin air layers, created by friction and viscous effects, on STL of finite panels.

ACKNOWLEDGMENT

A.D. is a Doctoral Fellow of the Research Foundation—Flanders (FWO—Vlaanderen).

[1]L. L. Beranek and G. A. Work, "Sound transmission through multiple structures containing flexible blankets," J. Acoust. Soc. Am. **21**, 419–428 (1949).
[2]K. A. Mulholland, H. D. Parbrook, and A. Cummings, "The transmission loss of double panels," J. Sound Vib. **6**, 324–334 (1967).
[3]A. London, "Transmission of reverberant sound through double walls," J. Acoust. Soc. Am. **22**, 270–279 (1950).
[4]F. Fahy, *Sound and Structural Vibration. Radiation, Transmission and Response* (Academic Press Limited, London, 1985), Chap. 4.
[5]A. C. K. Au and K. P. Byrne, "On the insertion losses produced by plane acoustic lagging structures," J. Acoust. Soc. Am. **82**, 1325–1333 (1987).
[6]W. Lauriks, P. Mees, and J. F. Allard, "The acoustic transmission through layered systems," J. Sound Vib. **155**, 125–132 (1992).
[7]A. J. Price and M. J. Crocker, "Sound transmission through double panels using statistical energy analysis," J. Acoust. Soc. Am. **47**, 683–693 (1970).
[8]R. J. M. Craik, *Sound Transmission Through Buildings Using Statistical Energy Analysis* (Gower, England, 1996), Chap. 7.
[9]R. J. M. Craik and R. S. Smith, "Sound transmission through double leaf lightweight partitions part I: Airborne sound," Appl. Acoust. **61**, 223–245 (2000).
[10]R. Panneton and N. Atalla, "Numerical prediction of sound transmission through finite multilayer systems with poroelastic materials," J. Acoust. Soc. Am. **100**, 346–354 (1996).
[11]F. C. Sgard, N. Atalla, and J. Nicolas, "A numerical model for the low frequency diffuse sound transmission loss of double-wall sound barriers with elastic porous linings," J. Acoust. Soc. Am. **108**, 2865–2872 (2000).
[12]L. Gagliardini, J. Roland, and J. L. Guyader, "The use of a functional basis to calculate acoustic transmission between rooms," J. Sound Vib. **145**, 457–478 (1991).
[13]W. Desmet, P. Sas, and D. Vandepitte, "An indirect Trefftz method for the steady-state dynamic analysis of coupled vibro-acoustic systems," Comp. Assist. Mech. Eng. Sc. **8**, 271–288 (2001).
[14]J. Brunskog, "The influence of finite cavities on the sound insulation of double-plate structures," J. Acoust. Soc. Am. **117**, 3727–3739 (2005).
[15]F. X. Xin, T. J. Lu, and C. Q. Chen, "Vibroacoustic behavior of clamp mounted double-panel partition with enclosure air cavity," J. Acoust. Soc. Am. **124**, 3604–3612 (2008).
[16]P. Jean and J. Rondeau, "A simple decoupled modal calculation of sound transmission between volumes," Acust. Acta Acust. **88**, 924–933 (2002).
[17]V. Hongisto, "Sound insulation of double panels—comparison of existing prediction models," Acust. Acta Acust. **92**, 61–78 (2006).
[18]T. Önsay, "Effects of layer thickness on the vibration response of a plate-fluid layer system," J. Sound Vib. **163**, 231–259 (1993).
[19]T. G. H. Basten, P. J. M. van der Hoogt, R. M. E. J. Spiering, and H. Tijdeman, "On the acousto-elastic behaviour of double-wall panels with a viscothermal air layer," J. Sound Vib. **243**, 699–719 (2001).
[20]T. G. H. Basten, "Noise reduction by viscothermal acousto-elastic interaction in double wall panels," Ph.D. thesis, University of Twente, Enschede, The Netherlands, 2001.
[21]A. Akrout, C. Karra, L. Hammami, and M. Haddar, "Viscothermal fluid effects on vibro-acoustic behaviour of double elastic panels," Int. J. Mech. Sci. **50**, 764–773 (2008).
[22]A. Akrout, L. Hammami, M. B. Tahar, and M. Haddar, "Vibro-acoustic behaviour of laminated double glazing enclosing a viscothermal fluid cavity," Appl. Acoust. **70**, 82–96 (2009).
[23]J. Allard and N. Atalla, *Propagation of Sound in Porous Media. Modelling Sound Absorbing Materials*, 2nd ed. (Wiley & Sons, Ltd, Chichester, 2009), Chap. 11.
[24]B. Brouard, D. Lafarge, and J. F. Allard, "A general method of modelling sound propagation in layered media," J. Sound Vib. **183**, 129–142 (1995).
[25]J. S. Bolton, N.-M. Shau, and Y. Kang, "Sound transmission through multi-panel structures lined with elastic porous materials," J. Sound Vib. **191**, 317–347 (1996).
[26]B. Sharp, "Prediction methods for the sound transmission of building elements," Noise Control Eng. J. **11**, 5363 (1978).
[27]H. Kang, J. Ih, J. Kim, and H. Kim, "Prediction of sound transmission loss through multilayered panels by using Gaussian distribution of directional incident energy," J. Acoust. Soc. Am. **107**, 1413–1420 (2000).
[28]M. Villot, C. Guigou, and L. Gagliardini, "Predicting the acoustical radiation of finite size multi-layered structures by applying spatial windowing on infinite structures," J. Sound Vib. **245**, 433–455 (2001).
[29]S. Kurra and D. Arditi, "Determination of sound transmission loss of multilayered elements part 1: Predicted and measured results," Acust. Acta Acust. **87**, 582–591 (2001).
[30]A. Osipov, P. Mees, and G. Vermeir, "Low-frequency airborne sound transmission through single partitions in buildings," Appl. Acoust. **52**, 273–288 (1997).
[31]A. Dijckmans, G. Vermeir, and W. Lauriks, "A wave based model to predict the airborne and structure-borne sound insulation of finite-sized multilayered structures," in *Proceedings of the International Conference on Acoustics NAG/DAGA 2009*, Rotterdam, The Netherlands (2009), pp. 478–481.
[32]L. Cremer, M. Heckl, and B. A. T. Petersson, *Structure-Borne Sound: Structural Vibrations and Sound Radiation at Audio Frequencies*, 3rd ed. (Springer, Berlin, 2005), Chap. 3.
[33]A. Dijckmans, G. Vermeir, and J. W. Niggebrugge, "Optimization of the acoustic performances of lightweight sandwich roof elements," in *Proceedings of Inter-Noise 2009*, Paper No. 271, Ottawa, Canada (2009).
[34]J.-D. Chazot and J.-L. Guyader, "Prediction of transmission loss of double panels with a patch-mobility method," J. Acoust. Soc. Am. **121**, 267–278 (2007).
[35]T. E. Vigran, "Predicting the sound reduction index of finite size specimen by a simplified spatial windowing technique," J. Sound Vib. **325**, 507–512 (2009).
[36]J. L. Davy, "The improvement of a simple theoretical model for the prediction of the sound insulation of double leaf walls," J. Acoust. Soc. Am. **127**, 841–849 (2010).